Proceedings of the EuroGNC 2013, 2nd CEAS Specialist Conference
on Guidance, Navigation & Control, Delft University of Technology,
Delft, The Netherlands, April 10-12, 2013

Space-borne Geolocation with a Quasi-planar Satellite Cluster

Noam Leiter* and Pini Gurfil†
Technion—Israel Institute of Technology, Haifa 32000, Israel

Space-borne geolocation aims at determining the Earth coordinates of a terrestrial emitter. Whereas algorithms for space-borne geolocation have been presented before, this study provides a theoretical basis for achieving optimal positioning performance based on sequential time difference of arrival measurements with a satellite cluster, while solving for the initial position ambiguity through recursive filtering techniques.

I. Introduction

Time Difference of Arrival (TDOA) positioning, also known as a hyperbolic fix, is part of a larger group of passive positioning methods. Such methods have numerous applications ranging from indoor robot navigation systems, through underwater acoustic positioning, to the Deep Space Network for tracking interplanetary spacecraft.

Various techniques have been developed for geolocating a single source using several receivers. Foy [1] introduced the Iterative Least Squares (ILS) method that was followed by several closed-form solutions proposed by Friedlander [2], Smith and Abel [3] and others. Modern methods, such as genetic algorithms [4] were developed as well. In order to solve for the three unknown emitter coordinates, all methods must use a minimum of three non-trivial TDOA measurements. In geolocation problems, the emitter is located on the geoid and the added constrain allows to solve for the emitter position with two TDOA measurements. Ho and Chan [5] presented an analytic solution with two TDOA measurements obtained by a three satellite formation, with a possible ambiguity of several solutions. Based on this method, we derive an iterative method for geolocation with a two satellite formation.

When several pulses, emitted from the same source, are available, a minimum of two receivers, moving relative to the source, could produce a sequence of TDOA measurements. Various positioning techniques could then be applied, such as an Extended Kalman Filter (EKF) [6], Unscented Kalman Filter (UKF) [7, 8] and Gaussian Measurement Mixture (GMM) [9]. All the methods must address the non-linearity of TDOA measurements and the possible ambiguity in the initial estimate which is critical for the convergence of the estimator. We present a sequential method for solving the initial ambiguity.

The positioning accuracy depends on the quality of the measurements and the geometry of the sensors [10]. The positioning accuracy limits will be presented. A quasi-planar satellite formation is an extremely poor geometry for geolocation, however it is beneficial for long term formation keeping [11] and hence the case study for this work.

*Graduate Student, Faculty of Aerospace Engineering, noaml@technion.ac.il.
†Associate Professor, Faculty of Aerospace Engineering, pgurfil@technion.ac.il.

II. System Model

A. Beacon Model

The beacon is assumed to be static in the Earth-Centered Earth-Fixed (ECEF) frame $\mathscr{F}$:

$$[\dot{\mathbf{s}}_0]_{\mathscr{F}} = \mathbf{0} \tag{1}$$

Relative to an Earth-Centered Inertial (ECI) frame the beacon dynamics are:

$$\dot{\mathbf{s}}_0 = [\boldsymbol{\Omega}_\oplus \times] \, \mathbf{s}_0 \tag{2}$$

where $\boldsymbol{\Omega}_\oplus$ is Earth's angular velocity vector.

B. Satellite Model

The cluster positions $\{\mathbf{s}_i\}_{i=1}^N$ are estimated in the on-board navigation computers. The navigation errors are assumed to be stationary and uncorrelated and modeled as Gaussian white noise signals:

$$\tilde{\mathbf{s}}_i = \mathbf{s}_i + \delta\mathbf{s}_i \tag{3}$$

$$\delta\mathbf{s}_i \sim \mathcal{N}(\mathbf{0}, R_s) \tag{4}$$

$$E\left[\delta\mathbf{s}_i \delta\mathbf{s}_j^T\right] = R_s \cdot \delta_{ij} \tag{5}$$

where δ_{ij} is the Kronecker delta:

$$\delta_{ij} = \begin{cases} 1 & i = j \\ 0 & i \neq j \end{cases} \tag{6}$$

A difference vector is defined for each pair of satellites in the cluster,

$$\mathbf{s}_{ji} \triangleq \mathbf{s}_j - \mathbf{s}_i \tag{7}$$

and a line of sight (LOS) vector to the beacon is defined for each of the satellites:

$$\mathbf{s}_{i0} \triangleq \mathbf{s}_i - \mathbf{s}_0 \tag{8}$$

C. TDOA Measurement Model

In this study each of the satellites performs a Time-of-Arrival (TOA) measurement $\tilde{t}_i$ and the TDOAs are obtained from the differences[a]. The TOA model considered hereafter is:

$$\tilde{t}_i = \frac{1}{c}\sqrt{\mathbf{s}_{i0}^T \mathbf{s}_{i0}} + t_0 + v_i \tag{9}$$

where c is the speed of light, t_0 is the (unknown) time of emission and v_i is the measurement error.

[a]If the TDOAs are obtained with some cross-correlation scheme, a different measurement model should be used.

1. Clock Bias Model

The measurement error is a combination of the on-board clock bias $b_i(t)$ sampled at the time of arrival t_i and the pulse detection error ε_i:

$$v_i(t_i) = b_i(t_i) + \varepsilon_i \tag{10}$$

The behavior of a clock bias could be modeled as a first-order Gauss-Markov process [12]:

$$\begin{bmatrix} \dot{b}(t) \\ \dot{d}(t) \end{bmatrix} = \begin{bmatrix} 0 & 1 \\ 0 & -\tau_d^{-1} \end{bmatrix} \begin{bmatrix} b(t) \\ d(t) \end{bmatrix} + \begin{bmatrix} 0 \\ \eta_d(t) \end{bmatrix} \tag{11}$$

where $d(t)$ is the clock drift, τ_d is the drift time constant and $\eta_d(t)$ is white Gaussian noise with power spectral density q_d:

$$E[\eta_d(t)] = 0 \quad , \qquad E[\eta_d(t)\,\eta_d(t')] = q_d \cdot \delta(t - t') \tag{12}$$

The on-board clock is assumed to be synchronized with GNNS time updates, (e.g, GPS 1-pps signal):

$$b(t_k) \sim \mathcal{N}\left(0, \sigma_b^2\right) \tag{13}$$

where $t_k = k \cdot \Delta t$ is the update time, with an update time interval Δt, and σ_b is the standard deviation of the steady state synchronization error. The dispersion of the bias variance p_b between updates is [12]:

$$p_b(\tau) = \sigma_b^2 + \frac{q_d \tau_d^3}{2}\left[2\frac{\tau}{\tau_d} + 4\left(1 - \exp\left\{-\frac{\tau}{\tau_d}\right\}\right) + \left(1 - \exp\left\{-\frac{2\tau}{\tau_d}\right\}\right)^2\right] \tag{14}$$

where $\tau \triangleq t - t_k$. For short time updates, $\Delta t \ll \tau_d$, p_b could be approximated:

$$p_b(\tau) \approx \sigma_b^2 + q_b \cdot \tau \quad , \qquad q_b \triangleq 3 q_d \tau_d^2 \ , \tag{15}$$

therefore, for a given time of arrival $t \in [t_k, t_k + \Delta t]$ the bias is normally distributed:

$$b(t)\,|t \sim \mathcal{N}\left(0, \sigma_b^2 + q_b(t - t_k)\right) \tag{16}$$

Without any prior information on the time of emission the TOA is uniformly distributed:

$$t \sim \mathcal{U}[t_k, t_k + \Delta t] \tag{17}$$

The distribution of the sampled clock bias is:

$$f(b) = \int_0^{\Delta t} f(b(\tau)\,|\tau)\, f(\tau)\, d\tau = \frac{1}{\Delta t}\int_0^{\Delta t} f(b(\tau)\,|\tau)\, d\tau \tag{18}$$

where

$$f(b(\tau)\,|\tau) \approx \frac{1}{\sqrt{2\pi\left(\sigma_b^2 + q_b\tau\right)}} \exp\left\{-\frac{1}{2}\frac{b^2}{\sigma_b^2 + q_b\tau}\right\} \tag{19}$$

The resulting sampled bias distribution is

$$f\left(\hat{b}\right) = \frac{\sqrt{\frac{2}{\pi}}}{(\alpha_b^2-1)}\left[\alpha_b \cdot \exp\left\{-\frac{\hat{b}^2}{2\alpha_b^2}\right\} - \exp\left\{-\frac{\hat{b}^2}{2}\right\}\right] + \frac{\hat{b}}{(\alpha_b^2-1)}\left[\operatorname{erf}\left\{\frac{\hat{b}}{\sqrt{2}\alpha_b}\right\} - \operatorname{erf}\left\{\frac{\hat{b}}{\sqrt{2}}\right\}\right] \tag{20}$$

where $\hat{b} = \frac{b}{\sigma_b}$ is the normalized bias, and

$$\alpha_b^2 \triangleq 1 + \frac{q_b \Delta t}{\sigma_b^2} \tag{21}$$

The sampled bias distribution is not Gaussian, however it could we approximated with a matched Gaussian:

$$g\left(\hat{b}, k^*\right) = \frac{\exp\left\{-\frac{1}{2}\frac{\hat{b}^2}{k^*}\right\}}{\sqrt{2\pi k^*}} \tag{22}$$

where $k^* \in [1, \alpha_b^2]$ is the solution to the least squares optimization:

$$k^* = \arg\min_k \left\{\varepsilon_k^2\right\} \tag{23}$$

with

$$\varepsilon_k^2 = \int_{-\infty}^{\infty}\left[g\left(\hat{b}, k\right) - f\left(\hat{b}\right)\right]^2 d\hat{b} \tag{24}$$

Under the matched Gaussian approximation the sampled bias at TOA is normally distributed

$$b_i\left(t_i\right) \sim \mathcal{N}\left(0, k^*\sigma_b^2\right) \tag{25}$$

The full derivation of the sampled bias distribution $f\left(\hat{b}\right)$ and the matched Gaussian $g\left(\hat{b}, k\right)$ is provided in the appendix.

Relative to the on-board clock time, the pulse detection error is assumed to be a zero mean i.i.d Gaussian process:

$$\varepsilon_i \sim \mathcal{N}\left(0, \sigma_\varepsilon^2\right), \tag{26}$$

therefore, the TOA measurement error could be modeled as white Gaussian noise:

$$v_i \sim \mathcal{N}\left(0, \sigma_t^2\right) \tag{27}$$

where

$$\sigma_t^2 = \sigma_\epsilon^2 + k^*\sigma_b^2 \tag{28}$$

2. Incorporating Navigation Estimates

We consider a system where the navigation filter and the geolocation algorithm are separated, i.e., the navigation estimates enter the geolocation algorithm as an input and not as part of the state. This model induces an additional measurement error as seen in the expansion of $\tilde{t}_i$ to first order in $\delta\mathbf{s}_i$ assuming $\|\delta\mathbf{s}_i\| \ll \|\mathbf{s}_{i0}\|$:

$$\tilde{t}_i \approx \frac{1}{c}\sqrt{\tilde{\mathbf{s}}_{i0}^T\tilde{\mathbf{s}}_{i0}} + t_0 + \mathbf{h}_i^T\delta\mathbf{s}_i + v_i \tag{29}$$

where $\tilde{\mathbf{s}}_{i0} = \tilde{\mathbf{s}}_i - \mathbf{s}_0$ and

$$\mathbf{h}_i = \left[\frac{\partial \tilde{t}_i}{\partial \mathbf{s}_i}\right]^T_{\mathbf{s}_i=\tilde{\mathbf{s}}_i} = \frac{1}{c}\frac{\tilde{\mathbf{s}}_{i0}}{\sqrt{\tilde{\mathbf{s}}_{i0}^T\tilde{\mathbf{s}}_{i0}}} \tag{30}$$

The total TOA measurement error is:

$$\delta t_i = \mathbf{h}_i^T \delta \mathbf{s}_i + v_i \tag{31}$$

and the TOA covariance is:

$$R_t = \mathrm{cov}\left\{\delta t_i\right\} = \mathbf{h}_i^T R_s \mathbf{h}_i + \sigma_t^2 \tag{32}$$

The cluster TDOAs are combined to a Range-Differences (RDs) vector:

$$\tilde{\mathbf{r}} = c\left[\tilde{t}_2 - \tilde{t}_1, \tilde{t}_3 - \tilde{t}_1, \ldots, \tilde{t}_N - \tilde{t}_1\right]^T \tag{33}$$

and the RDs covariance $R = \mathrm{cov}\left\{\tilde{\mathbf{r}}\right\}$ is:

$$R = c^2\mathbf{h}_1^T R_s \mathbf{h}_1 \cdot \underline{1}_{d_r}\underline{1}_{d_r}^T + c^2 \begin{bmatrix} \mathbf{h}_2^T \\ \vdots \\ \mathbf{h}_N^T \end{bmatrix} R_s \begin{bmatrix} \mathbf{h}_2 & \cdots & \mathbf{h}_N \end{bmatrix} + c^2\sigma_t^2 \cdot \left[I_{d_r\times d_r} + \underline{1}_{d_r}\underline{1}_{d_r}^T\right] \tag{34}$$

where $d_r = N-1$ and $\underline{1}_{d_r}^T \triangleq \begin{bmatrix} 1 & 1 & \cdots & 1 \end{bmatrix}_{1\times d_r}$.

3. TDOA Fisher Information Matrix

The Fisher information matrix (FIM) of the RDs measurement is:

$$J_k = E\left[\frac{\partial \mathcal{L}\left(\mathbf{z},\boldsymbol{\theta}\right)}{\partial \boldsymbol{\theta}}^T \frac{\partial \mathcal{L}\left(\mathbf{z},\boldsymbol{\theta}\right)}{\partial \boldsymbol{\theta}} | \boldsymbol{\theta}\right] = \int \frac{\partial \mathcal{L}\left(\mathbf{z},\boldsymbol{\theta}\right)}{\partial \boldsymbol{\theta}}^T \frac{\partial \mathcal{L}\left(\mathbf{z},\boldsymbol{\theta}\right)}{\partial \boldsymbol{\theta}} f\left(\mathbf{z}|\boldsymbol{\theta}\right) d\mathbf{z} \tag{35}$$

where $\boldsymbol{\theta}$ is the beacon position, and $\mathbf{z}$ is the RDs vector

$$\boldsymbol{\theta} \triangleq \mathbf{s}_0 \quad , \qquad \mathbf{z} \triangleq \tilde{\mathbf{r}} \ , \tag{36}$$

and where $\mathcal{L}\left(\mathbf{z},\boldsymbol{\theta}\right)$ is the log-likelihood function

$$\mathcal{L}\left(\mathbf{z},\boldsymbol{\theta}\right) = \log\left\{f\left(\mathbf{z}|\boldsymbol{\theta}\right)\right\}$$

For unbiased measurements with additive Gaussian noise the FIM is:

$$J_k\left(\boldsymbol{\theta}\right) = H\left(\boldsymbol{\theta}\right)^T R^{-1} H\left(\boldsymbol{\theta}\right) + \frac{1}{2}\Delta_k\left(\boldsymbol{\theta}\right) \tag{37}$$

where

$$H\left(\boldsymbol{\theta}\right) = \left.\frac{\partial \tilde{\mathbf{r}}}{\partial \mathbf{s}_0}\right|_{\mathbf{s}_0=\boldsymbol{\theta}} = \begin{bmatrix} \mathbf{h}_1^T - \mathbf{h}_2^T \\ \vdots \\ \mathbf{h}_1^T - \mathbf{h}_N^T \end{bmatrix}_{\mathbf{s}_0=\boldsymbol{\theta}} \tag{38}$$

$\Delta_k(\boldsymbol{\theta})$ is :

$$[\Delta_k(\boldsymbol{\theta})]_{mn} = \left[R^{-1}\right]_{ab} \frac{\partial R_{bc}}{\partial \theta_m} \left[R^{-1}\right]_{cd} \frac{\partial R_{da}}{\partial \theta_n} \tag{39}$$

with index summation convention

$$a, b, c, d = 1, 2, \ldots, N-1 \quad , \qquad m, n = 1, 2, \ldots, N \tag{40}$$

:

where

$$R_{ab} = c^2 \mathbf{h}_1^T R_s \mathbf{h}_1 + c^2 \mathbf{h}_{a+1}^T R_s \mathbf{h}_{b+1} + c^2 \sigma_t^2 \cdot [1 + \delta_{ab}] \tag{41}$$

$$\frac{\partial R_{bc}}{\partial \theta_m} = \left[\frac{\partial R_{ab}}{\partial \mathbf{s}_0}\right]_m \tag{42}$$

$$\frac{\partial R_{ab}}{\partial \mathbf{s}_0} = 2c^2 \mathbf{h}_1^T R_s \frac{\partial \mathbf{h}_1}{\partial \mathbf{s}_0} + c^2 \mathbf{h}_{a+1}^T R_s \frac{\partial \mathbf{h}_{b+1}}{\partial \mathbf{s}_0} + c^2 \mathbf{h}_{b+1}^T R_s \frac{\partial \mathbf{h}_{a+1}}{\partial \mathbf{s}_0} \tag{43}$$

$$\frac{\partial \mathbf{h}_m}{\partial \mathbf{s}_0} = \frac{1}{c} \left(\frac{\mathbf{s}_{m0} \mathbf{s}_{m0}^T}{\left(\mathbf{s}_{m0}^T \mathbf{s}_{m0}\right)^{\frac{3}{2}}} - \frac{I}{\sqrt{\mathbf{s}_{m0}^T \mathbf{s}_{m0}}} \right) \tag{44}$$

III. Initialization Methods

An ideal RD measurement

$$r_{ij} = \|\mathbf{s}_{i0}\| - \|\mathbf{s}_{j0}\| , \tag{45}$$

is a compact form of the hyperboloid quadric:

$$(\mathbf{s}_0 - \mathbf{c}_{ij})^T Q (\mathbf{s}_0 - \mathbf{c}_{ij}) = 1 \tag{46}$$

with foci at $\mathbf{s}_i$ and $\mathbf{s}_j$, where

$$\mathbf{c}_{ij} \triangleq \frac{\mathbf{s}_i + \mathbf{s}_j}{2} \quad , \qquad Q \triangleq \left(\frac{\mathbf{s}_{ij}^T \mathbf{s}_{ij} - r_{ij}^2}{4} \right)^{-1} \left[\frac{\mathbf{s}_{ij} \mathbf{s}_{ij}^T}{r_{ij}^2} - I \right] . \tag{47}$$

Applying the reverse triangle inequality on Eq. (45) we get:

$$|r_{ij}| \leq \|\mathbf{s}_{ij}\| \tag{48}$$

therefore the signature of Q is $(-,-,+)$ and it represents a two-sheet hyperboloid of revolution about $\mathbf{s}_{ij}$.

Given three RDs, a hyperbolic fix of the beacon $\mathbf{s}_0$ is one of the intersection points of the three RD hyperboloids. In geolocation problems the beacon is known to be on the surface of Earth, therefore, the position could be obtained with two RDs from the intersection of the two RD hyperboloids and Earth's surface constrain.

A. Initialization with three satellites

1. *Ho and Chan's method*

For a formation of three satellites, including a leader $\mathbf{s}_1$, and two followers $\mathbf{s}_2$ and $\mathbf{s}_3$, an exact solution has been presented by Ho and Chan [5], assuming a spherical Earth. The derivation of the solution is described here for completeness. The three satellites produce two RDs from a single pulse:

$$r_{21} = \|\mathbf{s}_{20}\| - \|\mathbf{s}_{10}\| \quad , \qquad r_{31} = \|\mathbf{s}_{30}\| - \|\mathbf{s}_{10}\| \tag{49}$$

which can be rearranged into:

$$r_{21}^2 + 2r_{21}r_1 + \mathbf{s}_1^T\mathbf{s}_1 - \mathbf{s}_2^T\mathbf{s}_2 = -2\mathbf{s}_{21}^T\mathbf{s}_0 \tag{50}$$

$$r_{31}^2 + 2r_{31}r_1 + \mathbf{s}_1^T\mathbf{s}_1 - \mathbf{s}_3^T\mathbf{s}_3 = -2\mathbf{s}_{31}^T\mathbf{s}_0 \tag{51}$$

where

$$r_1 \triangleq \|\mathbf{s}_{10}\| \tag{52}$$

The spherical surface constrain is:

$$\mathbf{s}_0^T\mathbf{s}_0 = r_\oplus^2 \tag{53}$$

where $r_\oplus$ is the equatorial Earth radius. Eq. (52) and (53) produce a third equation for r_1:

$$r_1^2 = \mathbf{s}_{10}^T\mathbf{s}_{10} = r_\oplus^2 + \mathbf{s}_1^T\mathbf{s}_1 - 2\mathbf{s}_1^T\mathbf{s}_0 \tag{54}$$

Equations (50), (51) and (54) are combined to a linear system, where the beacon coordinates are a function of a single unknown parameter r_1:

$$\mathbf{s}_0 = A^{-1}\mathbf{b}\,(r_1) \tag{55}$$

where

$$A = -2\begin{bmatrix} \mathbf{s}_1 & \mathbf{s}_{21} & \mathbf{s}_{31} \end{bmatrix}^T \tag{56}$$

The vector $\mathbf{b}$ is a function of the unknown parameter r_1:

$$\mathbf{b} = \begin{bmatrix} r_1^2 - r_\oplus^2 - \mathbf{s}_1^T\mathbf{s}_1 \\ r_{21}^2 + 2r_{21}r_1 - (2\mathbf{s}_1 + \mathbf{s}_{21})^T\mathbf{s}_{21} \\ r_{31}^2 + 2r_{31}r_1 - (2\mathbf{s}_1 + \mathbf{s}_{31})^T\mathbf{s}_{31} \end{bmatrix} = \mathbf{b}_2 r_1^2 + \mathbf{b}_1 r_1 + \mathbf{b}_0 \tag{57}$$

where

$$\mathbf{b}_2 = \begin{bmatrix} 1 & 0 & 0 \end{bmatrix}^T \quad , \quad \mathbf{b}_1 = \begin{bmatrix} 0 & 2r_{21} & 2r_{31} \end{bmatrix}^T \quad , \quad \mathbf{b}_0 = \begin{bmatrix} -r_\oplus^2 - \mathbf{s}_1^T\mathbf{s}_1 \\ r_{21}^2 - (2\mathbf{s}_1 + \mathbf{s}_{21})^T\mathbf{s}_{21} \\ r_{31}^2 - (2\mathbf{s}_1 + \mathbf{s}_{31})^T\mathbf{s}_{31} \end{bmatrix} \tag{58}$$

The solution for r_1 is obtained from reapplying the constraint Eq. (53):

$$\mathbf{b}^T A^{-T} A^{-1}\mathbf{b} = r_\oplus^2 \tag{59}$$

which is a quartic of r_1:

$$f(r_1) = \mathbf{b}^T W_A \mathbf{b} - r_\oplus^2 = k_4 \cdot r_1^4 + k_3 \cdot r_1^3 + k_2 \cdot r_1^2 + k_1 \cdot r_1 + k_0 = 0 \tag{60}$$

where $W_A = A^{-T} A^{-1}$ and the quartic coefficients are:

$$\begin{aligned} k_4 &= \mathbf{b}_2^T W_A \mathbf{b}_2 & k_3 &= 2\mathbf{b}_2^T W_A \mathbf{b}_1 \\ k_2 &= 2\mathbf{b}_2^T W_A \mathbf{b}_0 + \mathbf{b}_1^T W_A \mathbf{b}_1 & & \\ k_1 &= 2\mathbf{b}_1^T W_A \mathbf{b}_0 & k_0 &= \mathbf{b}_0^T W_A \mathbf{b}_0 - r_\oplus^2 \end{aligned} \tag{61}$$

A solution could be obtained provided that A is full rank, applying the following conditions on the formation geometry:

$$\mathbf{s}_{21} \nparallel \mathbf{s}_{31} \quad , \quad \mathbf{s}_{21} \nparallel \mathbf{s}_1 \quad , \quad \mathbf{s}_{31} \nparallel \mathbf{s}_1 \tag{62}$$

2. Initial Ambiguity

The quartic $f(r_1)$ has up to four real positive roots. For a satellite formation $\|\mathbf{s}_1\| > \|\mathbf{s}_0\|$, therefore $r_1 \in [r_{min}, r_{max}]$. $r_{min} = \|\mathbf{s}_1\| - r_\oplus$ is the local altitude of $\mathbf{s}_1$ above the sphere and $r_{max} = \sqrt{\|\mathbf{s}_1\|^2 - r_\oplus^2}$ is the distance to the local horizon of $\mathbf{s}_1$. When two or more solutions are in the range $[r_{min}, r_{max}]$ there is an ambiguity in the initial beacon position. The condition for this depends on the cluster geometry with respect to the beacon. Each of the N_0 roots $\left\{r_1^{(i)}\right\}_{i=1}^{N_0} \in [r_{min}, r_{max}]$ corresponds to different positions: $\hat{\mathbf{s}}_0^{(i)}$, an estimate of the true beacon position or a phantom. These positions, as seen in Fig.1, are equivalent in the sense of the measurements, i.e., if the pulse was transmitted from either positions, the same TDOAs would have been measured in the formation. Only additional information could solve this ambiguity.

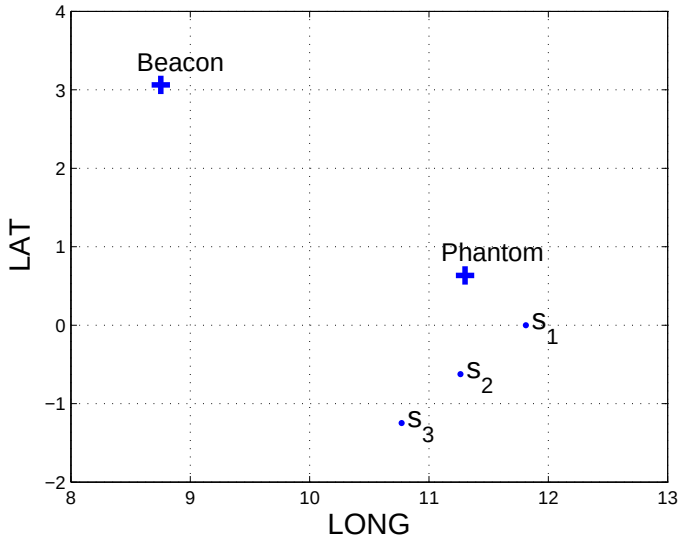

Figure 1: The geometry of target ambiguity with a quasi-planar formation

3. Non-Spherical Earth model

The spherical constraint in Eq.53 is a zero order Earth surface model with an error in the local radius increasing with the latitude up to about 20km at the poles. A more accurate model is the oblate sphere ellipsoid:

$$\mathbf{s}_0^T P_\oplus^{-1} \mathbf{s}_0 = r_\oplus^2 \tag{63}$$

where $P_\oplus$ is

$$P_\oplus = \begin{bmatrix} 1 & 0 & 0 \\ 0 & 1 & 0 \\ 0 & 0 & (1-f_\oplus)^2 \end{bmatrix}$$

and $f_\oplus$ is the flattening factor. With the ellipsoid constrain the exact solution in Eq.(55) could not be applied directly and the following iterative method is applied [5]:

1. The ellipsoid constrain is replaced with a sphere constrain:

$$\left(\hat{\mathbf{s}}_{0(k)}^{(i)}\right)^T \hat{\mathbf{s}}_{0(k)}^{(i)} = \left(\hat{r}_{L(k)}^{(i)}\right)^2 \tag{64}$$

   where $\hat{r}_{L(k)}^{(i)}$ is an estimate (after k iterations) of $r_L^{(i)}$, the local Earth radius at the position of $\mathbf{s}_{0(k)}^{(i)}$.

2. By replacing $r_\oplus$ with $\hat{r}_{L(k)}^{(i)}$, the exact method provides an estimate of $\hat{\mathbf{s}}_{0(k)}^{(i)}$. The local radius estimate is then updated for each of the N_0 initial estimates:

$$\hat{r}_{L(k+1)}^{(i)} = \sqrt{\frac{\left(\hat{\mathbf{s}}_{0(k)}^{(i)}\right)^T \hat{\mathbf{s}}_{0(k)}^{(i)}}{\left(\hat{\mathbf{s}}_{0(k)}^{(i)}\right)^T P_\oplus^{-1} \hat{\mathbf{s}}_{0(k)}^{(i)}}} r_\oplus \tag{65}$$

3. The iterations continue until convergence of $\hat{r}_{L(k)}^{(i)}$.

$r_L^{(i)}$ is bounded in the range:

$$r_L^{(i)} \in \left[(1-f_\oplus), 1\right] \cdot r_\oplus \tag{66}$$

and is initialized with the leader's local Earth radius:

$$\hat{r}_{L(0)}^{(i)} = \sqrt{\frac{\mathbf{s}_1^T \mathbf{s}_1}{\mathbf{s}_1^T P_\oplus^{-1} \mathbf{s}_1}} r_\oplus \tag{67}$$

4. Initial Estimate covariance

The covariance of $\hat{\mathbf{s}}_0^{(i)}$ is:

$$P_0^{(i)} = \mathrm{cov}\left\{\hat{\mathbf{s}}_0^{(i)}\right\} = \begin{bmatrix} H\left(\hat{\mathbf{s}}_0^{(i)}\right) \\ 2\left(\hat{\mathbf{s}}_0^{(i)}\right)^T P_\oplus^{-1} \end{bmatrix}^{-1} R_0\left(\hat{\mathbf{s}}_0^{(i)}\right) \begin{bmatrix} H\left(\hat{\mathbf{s}}_0^{(i)}\right) \\ 2\left(\hat{\mathbf{s}}_0^{(i)}\right)^T P_\oplus^{-1} \end{bmatrix}^{-T} \tag{68}$$

where

$$R_0 = \begin{bmatrix} R & 0_{2\times 1} \\ 0_{1\times 2} & 0 \end{bmatrix} \tag{69}$$

and where R is the RDs covariance as in Eq.34 for $N = 3$.

B. Initialization with two satellites

For a formation of two satellites, a leader $\mathbf{s}_1$, and a follower $\mathbf{s}_2$, the two necessary RDs could only be obtained from two pulses:

$$r_{21} = \|\mathbf{s}_{20}\| - \|\mathbf{s}_{10}\| \quad , \qquad r_{43} = \|\mathbf{s}_{40}\| - \|\mathbf{s}_{30}\| \tag{70}$$

where $\mathbf{s}_3$ and $\mathbf{s}_4$ are the positions of the leader and follower $\mathbf{s}_1$ and $\mathbf{s}_2$ at the TOA of the second pulse. The exact solution in Eq.(55) does not apply directly in this case, however we suggest the following modification:

$$\mathbf{s}_0 = A^{-1}\mathbf{b}\left(r_1, r_3\right) \tag{71}$$

where

$$r_3 = \|\mathbf{s}_{30}\| \tag{72}$$

and

$$A = -2\begin{bmatrix} \mathbf{s}_1^T \\ \mathbf{s}_{21}^T \\ \mathbf{s}_{43}^T \end{bmatrix} \quad , \qquad \mathbf{b} = \begin{bmatrix} r_1^2 - r_\oplus^2 - \mathbf{s}_1^T\mathbf{s}_1 \\ r_{21}^2 + 2r_{21}r_1 - \left(2\mathbf{s}_1 + \mathbf{s}_{21}\right)^T\mathbf{s}_{21} \\ r_{43}^2 + 2r_{43}r_3 - \left(2\mathbf{s}_3 + \mathbf{s}_{43}\right)^T\mathbf{s}_{43} \end{bmatrix} \tag{73}$$

By introducing the scalar $a > 0$:

$$a \triangleq \frac{r_3}{r_1} \tag{74}$$

the vector $\mathbf{b}$ in Eq.(71) is now a function of r_1 and a:

$$\mathbf{b}\left(r_1, a\right) = \mathbf{b}_2 r_1^2 + \mathbf{b}_1\left(a\right) r_1 + \mathbf{b}_0 \tag{75}$$

The quartic coefficients are as in Eq. (61) with:

$$\mathbf{b}_2 = \begin{bmatrix} 1 & 0 & 0 \end{bmatrix}^T \quad , \quad \mathbf{b}_1 = \begin{bmatrix} 0 & 2r_{21} & 2r_{43}\cdot a \end{bmatrix}^T \quad , \quad \mathbf{b}_0 = \begin{bmatrix} -r_\oplus^2 - \mathbf{s}_1^T\mathbf{s}_1 \\ r_{21}^2 - \left(2\mathbf{s}_1 + \mathbf{s}_{21}\right)^T\mathbf{s}_{21} \\ r_{43}^2 - \left(2\mathbf{s}_3 + \mathbf{s}_{43}\right)^T\mathbf{s}_{43} \end{bmatrix} \tag{76}$$

The following iterative method is then applied:

1. For a given a_k we solve the quartic $f\left(r_1, a_k\right) = 0$ and obtain $\left\{\mathbf{s}_{0(k)}^{(i)}\right\}_{i=1}^{N_0}$.

2. A consistent choice of $\mathbf{s}_{0(k)}^{(i)}$ is then used to obtain a_{k+1} for the next iteration:

$$a_{k+1} = \frac{\left\|\mathbf{s}_3 - \mathbf{s}_{0(k)}^{(i)}\right\|}{r_1\left(a_k\right)} \tag{77}$$

3. The iterations are performed until the convergence of a.

$\mathbf{s}_0$ is in the horizon of both $\mathbf{s}_1$ and $\mathbf{s}_3$, therefore a is bounded in the range:

$$a \in \left[\frac{\|\mathbf{s}_3\| - r_\oplus}{\sqrt{\|\mathbf{s}_1\|^2 - r_\oplus^2}}, \frac{\sqrt{\|\mathbf{s}_3\|^2 - r_\oplus^2}}{\|\mathbf{s}_1\| - r_\oplus} \right] \tag{78}$$

In the case that the two pulses are transmitted in an interval $\Delta T \ll \frac{\|\mathbf{s}_{21}\|}{\|\dot{\mathbf{s}}_1\|}$ we get $r_1 \approx r_3$, therefore we choose $a_0 = 1$ to initialize the algorithm.

If the ellipsoid constrain in Eq.(63) is used, combined iterations are performed for a and r_L. This combined iteration method provides the intersection points of two hyperboloids of revolution and an oblate sphere and has been shown to converge in simulations. A convergence analysis is subject for additional studies. Initializing with two satellites and two measurements does not solve the ambiguity problem as will be shown in the following results.

1. Initial Estimate covariance

The covariance of $\hat{\mathbf{s}}_0^{(i)}$ is:

$$P_0^{(i)} = \operatorname{cov}\left\{\hat{\mathbf{s}}_0^{(i)}\right\} = \begin{bmatrix} H\left(\hat{\mathbf{s}}_0^{(i)}\right) \\ 2\left(\hat{\mathbf{s}}_0^{(i)}\right)^T P_\oplus^{-1} \end{bmatrix}^{-1} R_0\left(\hat{\mathbf{s}}_0^{(i)}\right) \begin{bmatrix} H\left(\hat{\mathbf{s}}_0^{(i)}\right) \\ 2\left(\hat{\mathbf{s}}_0^{(i)}\right)^T P_\oplus^{-1} \end{bmatrix}^{-T} \tag{79}$$

where

$$H(\mathbf{s}_0) = \begin{bmatrix} \mathbf{h}_1^T - \mathbf{h}_2^T \\ \mathbf{h}_3^T - \mathbf{h}_4^T \end{bmatrix}, \tag{80}$$

$$R_0 = \begin{bmatrix} R_{21} & 0 & 0 \\ 0 & R_{43} & 0 \\ 0 & 0 & 0 \end{bmatrix} \tag{81}$$

and

$$\begin{aligned} R_{21} &= c^2 \mathbf{h}_1^T R_s \mathbf{h}_1 + c^2 \mathbf{h}_2^T R_s \mathbf{h}_2 + 2 \cdot c^2 \sigma_t^2 \\ R_{43} &= c^2 \mathbf{h}_3^T R_s \mathbf{h}_3 + c^2 \mathbf{h}_4^T R_s \mathbf{h}_4 + 2 \cdot c^2 \sigma_t^2 \end{aligned} \tag{82}$$

IV. Filtering Method

A. SMM-EKF with TDOA measurements

In the case that additional pulses are measured, the initial ambiguity could be resolved. For a sequential estimator we choose to apply a Static Multiple Model (SMM) scheme with N_0 hypothesis corresponding to the initial estimates $\left\{\mathbf{s}_0^{(i)}\right\}_{i=1}^{N_0}$ and covariances $\left\{P_0^{(i)}\right\}_{i=1}^{N_0}$:

$$\mathcal{M}_i = \left\{\hat{\mathbf{s}}_0^{(i)}(t_0), P_0\left(\hat{\mathbf{s}}_0^{(i)}\right), F_k^i, B_k^i, G_k^i, R_k^i, Q_k^i\right\} \tag{83}$$

The initial mode matched probabilities $\{\mu_i\}_{i=1}^{N_0}$ are chosen to reflect the equivalence of the phantom and the true target:

$$\mu_i = \frac{1}{N_0} \tag{84}$$

For each mode an extended Kalman filter (EKF) estimator is used with:

$$F_k^i = I \quad , \qquad B_k^i = G_k^i = Q_k^i = 0 \tag{85}$$

H_k^i and R_k^i are calculated according to Eq. (38) and Eq. (34) with $\mathbf{s}_0 = \hat{\mathbf{s}}_0^{(i)}$.
The SMM algorithm is described in the appendix.

B. Estimation Bounds

The FIM of the sequence of RDs is:

$$I_M = \sum_{k=1}^{M} J_k \tag{86}$$

where J_k is calculated according to Eq.(37). From I_M the Cramer-Rao lower bound (CRLB) could be obtained:

$$E\left[\left(\hat{\mathbf{s}}_0 - \mathbf{s}_0\right)^T \left(\hat{\mathbf{s}}_0 - \mathbf{s}_0\right) \mid \{\tilde{\mathbf{r}}_k\}_{k=1}^M\right] \geq \mathrm{tr}\left\{I_M^{-1}\right\} \tag{87}$$

The CRLB could only be obtained when I_M is full rank, and it does not incorporate constrains. In this study the target is constrained to the earth surface, and the initial FIM is singular, therefore, a constrained CRLB is used [13]:

$$E\left[\left(\hat{\mathbf{s}}_0 - \mathbf{s}_0\right)^T \left(\hat{\mathbf{s}}_0 - \mathbf{s}_0\right) \mid \{\tilde{\mathbf{r}}_k\}_{k=1}^M\right] \geq \mathrm{tr}\left\{U\left[U^T I_M U\right]^\dagger U^T\right\} \tag{88}$$

where $[]^\dagger$ denotes the Moore–Penrose pseudo-inverse and $U(\mathbf{s}_0)$ is an orthonormal basis of the null space of $R\left(\mathbf{s}_0\right)$, the normal space to the constrain at $\mathbf{s}_0$:

$$R\left(\mathbf{s}_0\right) U\left(\mathbf{s}_0\right) = \mathbf{0} \quad , \qquad U^T U = I \tag{89}$$

For the oblate sphere model the constrain is:

$$r\left(\mathbf{s}_0\right) = \mathbf{s}_0^T P_\oplus^{-1} \mathbf{s}_0 - r_\oplus^2 = 0 \tag{90}$$

therefore,

$$R\left(\mathbf{s}_0\right) = \frac{\partial r\left(\mathbf{s}_0\right)}{\partial \mathbf{s}_0} = \mathbf{s}_0^T P_\oplus^{-1} \tag{91}$$

U could be chosen to be the East-North subspace of the local East-North-Up (ENU) frame:

$$U = \left[\hat{\mathbf{u}}_1 \;\; \hat{\mathbf{u}}_2 \;\right] \tag{92}$$

where

$$\hat{\mathbf{u}}_1 = -\left[\hat{\mathbf{n}}\times\right]\hat{\mathbf{z}} \quad , \qquad \hat{\mathbf{u}}_2 = -\left[\hat{\mathbf{n}}\times\right]^2 \hat{\mathbf{z}} \tag{93}$$

and where $\hat{\mathbf{n}}\left(\mathbf{s}_0\right)$ is the local normal unit vector:

$$\hat{\mathbf{n}}\left(\mathbf{s}_0\right) = \frac{P_\oplus^{-1}\mathbf{s}_0}{\sqrt{\mathbf{s}_0^T P_\oplus^{-2} \mathbf{s}_0}} \tag{94}$$

The transformation from the ECEF frame $\mathcal{F}$ to the local ENU frame $\mathcal{L}$ is:

$$T_{\mathcal{F}2\mathcal{L}} = \left[\begin{array}{cc} U & \hat{\mathbf{n}} \end{array}\right]^T \tag{95}$$

V. Results

A. Setup

A three-satellite cluster is propagated along Keplerian orbits starting from the initial orbital elements:

$$\begin{aligned} \mathbf{e}_1 &= \{a_1, e_1, i_1, \omega_1, \Omega_1, \nu_1, M_1\} \\ \mathbf{e}_2 &= \{a_1, e_1, i_1, \omega_1, \Omega_1 + \varepsilon_2, \nu_1 + \phi_2, M_1\} \\ \mathbf{e}_3 &= \{a_1, e_1, i_1, \omega_1, \Omega_1 + \varepsilon_3, \nu_1 + \phi_3, M_1\} \end{aligned} \tag{96}$$

The leader $\mathbf{s}_1$ is on a circular orbit ($e_1 = 0$), while $\mathbf{s}_2$ and $\mathbf{s}_3$ are phased from $\mathbf{s}_1$ by small anomaly angles ϕ_2, $\phi_3 \ll 1$ and perturbed out of the plane by RAAN differences ε_2, $\varepsilon_3 \ll 1$. The distance between the satellites is chosen to be approximately $\|\mathbf{s}_{21}\| = \|\mathbf{s}_{32}\| \approx 100$km, from which we determine ϕ_2 and ϕ_3:

$$\phi_2 = -2 \cdot \sin^{-1}\left(\frac{\|\mathbf{s}_{21}\|}{2 \cdot a_1}\right) \quad , \qquad \phi_3 = 2 \cdot \phi_2 \tag{97}$$

All perturbing dynamics [14] are neglected along the examined 100 seconds. A beacon is positioned on Earth's surface in the horizon of the initial position of $\mathbf{s}_1$. The surface model used is the WGS-84 ellipsoid. The beacon transmits 10 consecutive pulses with a pulse repetition interval of $\Delta T = 10$sec. The Earth's spin vector is assumed to constant during the100 sec:

$$\mathbf{\Omega}_\oplus = [0, 0, \Omega_\oplus]^T \tag{98}$$

The covariance of the satellite position estimate is modeled as:

$$R_s = \sigma_s^2 \cdot I_{3\times 3} \tag{99}$$

All simulation setup parameters are given in Table 1.

Symbol	Value	Units	Description
$\Omega_\oplus$	$7.292 \cdot 10^5$	$\frac{rad}{sec}$	Earth's spin
$\mu_\oplus$	$3.986 \cdot 10^5$	$\frac{km^3}{sec^2}$	Earth's standard gravitational parameter
$r_\oplus$	6378.198	km	Earth's equatorial radius
Ω_1	0	deg	Leader's RAAN
ω_1	0	deg	Leader's argument of perigee
i_1	50	deg	Leader's inclination
a_1	7078.1	km	Leader's semi-major axis
e_1	0		Leader's eccentricity
M_1	0	deg	Leader's initial mean anomaly
ε_2	-0.0278	deg	$\mathbf{s}_2$ RAAN angle difference
ε_3	0	deg	$\mathbf{s}_3$ RAAN angle difference
σ_t	100	n sec	TOA measurement $1-\sigma$
σ_s	5	m	Satellite position $1-\sigma$ (per axis)

Table 1: Setup Values

B. Case study

We examine a beacon positioned in an intermediate initial range $r_1 = 1477$km, where $r_{max} \approx 3070$km and $r_{min} \approx 700$km. The scenario is examined twice, first with the three satellite formation, and second with only two of the three satellites, $\mathbf{s}_1$ and $\mathbf{s}_2$ taken from the same three satellite positions sequence. For both cases there is an initial ambiguity, as shown in Fig. 2.

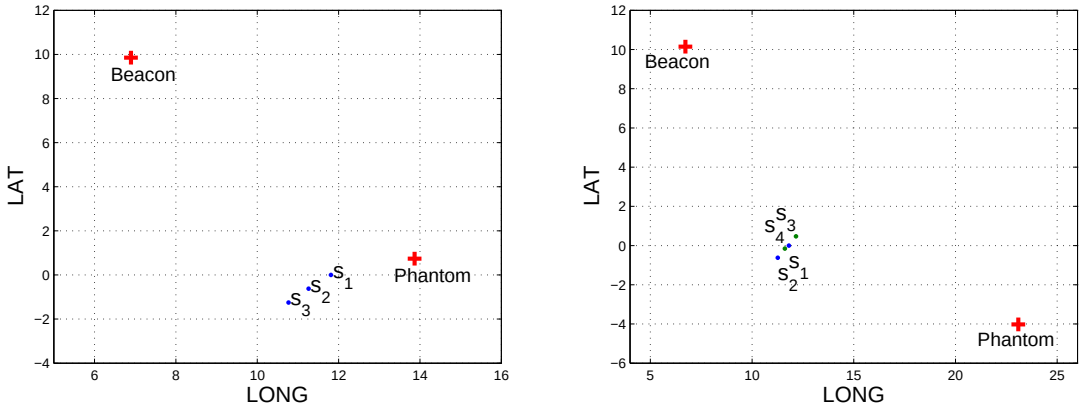

(a) Initialization with three satellites (b) Initialization with two satellites

Figure 2: Quasi-planar formation and target ambiguity

RMS results and averaged mode probabilities are calculated for each case based on 1000 Monte Carlo runs.

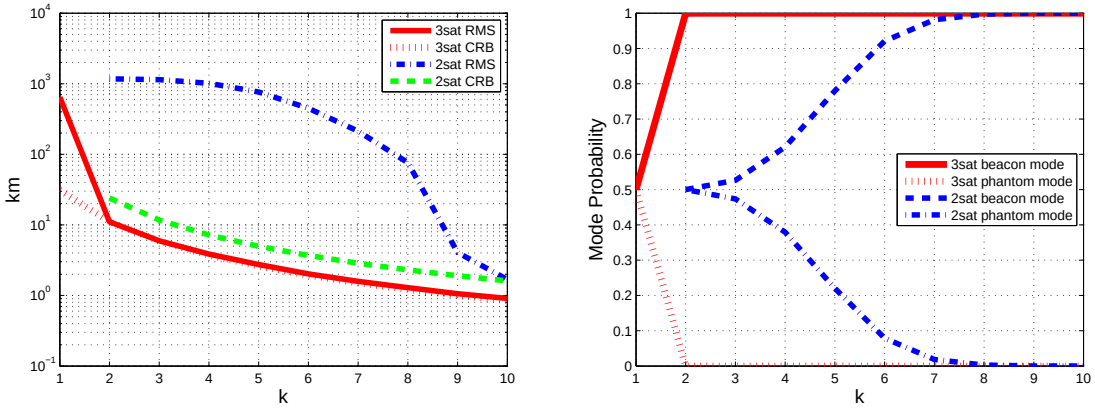

(a) Estimation RMS and CRLB (b) SMM mode probabilities

Figure 3: SMM Monte Carlo Results

As shown in Fig.3, the SMM processing the measurements of the three satellite formation (two RDs per pulse) achieves the constrained CRLB and identifies the true target with two pulses, where the two satellite SMM (one RD per pulse) identifies the true target after 8 pulses and achieves the CRLB only at the final pulse. The initial RMS error is hundreds of km because the SMM takes the midpoint between the true target and the phantom as the initial estimate. The final RMS error is 1km and 2km for the two an three satellite formations.

VI. Conclusions

We presented an initialization method with a two satellite formation and have demonstrated the usefulness of a combined initialization method with a SMM in solving the ambiguity problem. A Constrained CRLB has been contracted and Monte Carlo runs have shown the efficiency of the method. The proposed method can be implemented in real-time geolocation applications for two and three satellite formations.

References

1. Foy, W., "Position-location solutions by Taylor-series estimation," *IEEE Transactions on Aerospace and Electronic Systems*, , No. 2, 1976, pp. 187–194.

2. Friedlander, B., "A passive localization algorithm and its accuracy analysis," *IEEE Journal of Oceanic Engineering*, Vol. 12, No. 1, 1987, pp. 234–245.

3. Smith, J. and Abel, J., "Closed-form least-squares source location estimation from range-difference measurements," *IEEE Transactions on Acoustics, Speech and Signal Processing*, Vol. 35, No. 12, 1987, pp. 1661–1669.

4. Li, L. and Wei, F., "Position Estimation by Improved Genetic Algorithm for Hyperbolic Location," *14th IST Mobile & Wireless Communications*, 2005.

5. Ho, K. and Chan, Y., "Geolocation of a known altitude object from TDOA and FDOA measurements," *IEEE Transactions on Aerospace and Electronic Systems*, Vol. 33, No. 3, 1997, pp. 770–783.

6. Okello, N., Fletcher, F., Musicki, D., and Ristic, B., "Comparison of Recursive Algorithms for Emitter Localisation using TDOA Measurements from a Pair of UAVs," *IEEE Transactions on Aerospace and Electronic Systems*, Vol. 47, No. 3, 2011, pp. 1723–1732.

7. Savage, C., Cramer, R., and Schmitt, H., "TDOA geolocation with the unscented Kalman filter," *IEEE International Conference on Networking, Sensing and Control*, 2006, pp. 602–606.

8. Fletcher, F., Ristic, B., and Musicki, D., "Recursive estimation of emitter location using TDOA measurements from two UAVs," *10th International Conference on Information Fusion*, IEEE, 2007, pp. 1–8.

9. Musicki, D., Kaune, R., and Koch, W., "Mobile emitter geolocation and tracking using TDOA and FDOA measurements," *IEEE Transactions on Signal Processing*, Vol. 58, No. 3, 2010, pp. 1863–1874.

10. Lee, H., "A novel procedure for assessing the accuracy of hyperbolic multilateration systems," *IEEE Transactions on Aerospace and Electronic Systems*, , No. 1, 1975, pp. 2–15.

11. Gurfil, P., Herscovitz, J., and Pariente, M., "The SAMSON Project - Cluster Flight and Geolocation with Three Autonomous Nano-satellites," *26th AIAA/USU Conference on Small Satellites*, Salt Lake City, UT, USA, August 2012.

12. Carpenter, R. and Lee, T., "A Stable Clock Error Model Using Coupled First and Second Order Gauss-Markov Processes," *ai-solutions.com*, 2008.

13. Ben-Haim, Z. and Eldar, Y., "On the constrained Cramér–Rao bound with a singular Fisher information matrix," *Signal Processing Letters, IEEE*, 2009.

14. Alfriend, K., Vadali, S., Gurfil, P., How, J., and Breger, L., *Spacecraft formation flying: dynamics, control, and navigation*, Elsevier, 2010.

15. Bar-Shalom, Y., Li, X.-R., and Kirubarajan, T., *Estimation with Applications to Tracking and Navigation*, John Wiley & Sons, Inc., 2002, pp. 441–443.

Appendix 1- Sampled Clock Bias Model

The TOA conditioned bias is normal:

$$b\left(t\right)|t\sim\mathcal{N}\left(0,p_{b}\right) \tag{100}$$

where:

$$p_{b}\left(t\right)=\sigma_{b}^{2}+q_{b}\left(t-t_{k}\right) \tag{101}$$

The TOA is uniformly distributes:

$$t\sim\mathcal{U}\left[t_{k},t_{k}+\Delta t\right] \tag{102}$$

The conditioned bias pdf is

$$f\left(b\left(\tau\right)|\tau\right) = \frac{\exp\left\{-\frac{1}{2}\frac{b^{2}}{\sigma_{b}^{2}+q_{b}\tau}\right\}}{\sqrt{2\pi\left(\sigma_{b}^{2}+q_{b}\tau\right)}}=\frac{\exp\left\{-\frac{1}{2}\frac{b^{2}}{\rho_{b}\left(\tau\right)}\right\}}{\sqrt{2\pi\rho_{b}\left(\tau\right)}}$$

We define

$$\tau=t-t_{k}\sim\mathcal{U}\left[0,\Delta t\right] \tag{103}$$

and

$$\rho_{b}\left(\tau\right)\equiv\sigma_{b}^{2}+q_{b}\tau \tag{104}$$

The sampled bias pdf is calculated:

$$\begin{aligned}
f\left(b\right) &= \int_{0}^{\Delta t}f\left(b\left(\tau\right)|\tau\right)f\left(\tau\right)d\tau=\frac{1}{\Delta t}\int_{0}^{\Delta t}f\left(b\left(\tau\right)|\tau\right)d\tau\\
&= \frac{1}{q_{b}\Delta t}\int_{\sigma_{b}^{2}}^{\sigma_{b}^{2}+q_{b}\Delta t}\frac{\exp\left\{-\frac{1}{2}\frac{b^{2}}{\rho_{b}\left(\tau\right)}\right\}}{\sqrt{2\pi\rho_{b}\left(\tau\right)}}d\rho\\
&= \frac{1}{q_{b}\Delta t}\left[\sqrt{\frac{2\rho_{b}\left(\tau\right)}{\pi}}\cdot\exp\left\{-\frac{1}{2}\frac{b^{2}}{\rho_{b}\left(\tau\right)}\right\}+b\cdot\mathrm{erf}\left\{\frac{b}{\sqrt{2\rho_{b}\left(\tau\right)}}\right\}\right]_{0}^{\Delta t}\\
&= \frac{\sigma_{b}}{q_{b}\Delta t}\sqrt{\frac{2}{\pi}}\left[\sqrt{1+\frac{q_{b}\Delta t}{\sigma_{b}^{2}}}\cdot\exp\left\{-\frac{1}{2}\frac{b^{2}}{\sigma_{b}^{2}+q_{b}\Delta t}\right\}-\exp\left\{-\frac{1}{2}\frac{b^{2}}{\sigma_{b}^{2}}\right\}\right]+\\
&\quad+\frac{b}{q_{b}\Delta t}\left[\mathrm{erf}\left\{\frac{b}{\sqrt{2\left(\sigma_{b}^{2}+q_{b}\Delta t\right)}}\right\}-\mathrm{erf}\left\{\frac{b}{\sqrt{2\sigma_{b}^{2}}}\right\}\right]
\end{aligned}$$

The resulting sampled bias pdf is:

$$f\left(\hat{b}\right)=\frac{1}{\left(\alpha_{b}^{2}-1\right)}\left(\sqrt{\frac{2}{\pi}}\left[\alpha_{b}\cdot\exp\left\{-\frac{\hat{b}^{2}}{2\alpha_{b}^{2}}\right\}-\exp\left\{-\frac{\hat{b}^{2}}{2}\right\}\right]+\hat{b}\left[\mathrm{erf}\left\{\frac{\hat{b}}{\sqrt{2}\alpha_{b}}\right\}-\mathrm{erf}\left\{\frac{\hat{b}}{\sqrt{2}}\right\}\right]\right) \tag{105}$$

where $\hat{b}\equiv\frac{b}{\sigma_{b}}$ and

$$\alpha_{b}^{2}\equiv1+\frac{q_{b}\Delta t}{\sigma_{b}^{2}} \tag{106}$$

The matched Gaussian is

$$g\left(\hat{b},k\right)=\frac{\exp\left\{-\frac{1}{2}\frac{\hat{b}^{2}}{k}\right\}}{\sqrt{2\pi k}} \tag{107}$$

where

$$k \in \left[1, \alpha_b^2\right] \tag{108}$$

A least squares optimal matching is achieves with k^*:

$$k^* = \arg\min_k \left\{\varepsilon_k^2\right\} \tag{109}$$

where

$$\varepsilon_k^2 = \int_{-\infty}^{\infty} \left[g\left(\hat{b}, k\right) - f\left(\hat{b}\right)\right]^2 d\hat{b} \tag{110}$$

An extremum condition for the minimizing k:

$$\frac{\partial \varepsilon_k^2}{\partial k} = 2\int_{-\infty}^{\infty} \left[g\left(\hat{b}, k\right) - f\left(\hat{b}\right)\right] \frac{\partial g\left(\hat{b}, k\right)}{\partial k} d\hat{b} = 0$$

$$\frac{\partial g\left(\hat{b}, k\right)}{\partial k} = \frac{\exp\left\{-\frac{1}{2}\frac{\hat{b}^2}{k}\right\}}{\sqrt{2\pi k}} \frac{\hat{b}^2 - k}{2k^2} = \frac{\hat{b}^2 - k}{2k^2} g\left(\hat{b}, k\right)$$

$$\frac{\partial \varepsilon_k^2}{\partial k} = \int_{-\infty}^{\infty} \left[g\left(\hat{b}, k\right)^2 - g\left(\hat{b}, k\right) f\left(\hat{b}\right)\right] \frac{\hat{b}^2 - k}{k^2} d\hat{b} \tag{111}$$

The error gradient is nonlinear in k, therefore, the minimum problem could be solved iteratively, e.g., with a gradient search:

$$k^{(i+1)} = k^{(i)} - \gamma_k \cdot \frac{\partial \varepsilon_k^2}{\partial k} \tag{112}$$

The search is initialized with $k^{(0)} = 1$. γ_k is the step size. The bias distributions are presented in Fig.4 as well as the comparison of the sampled bias pdf and the matched Gaussian for $\alpha_b = 4$.

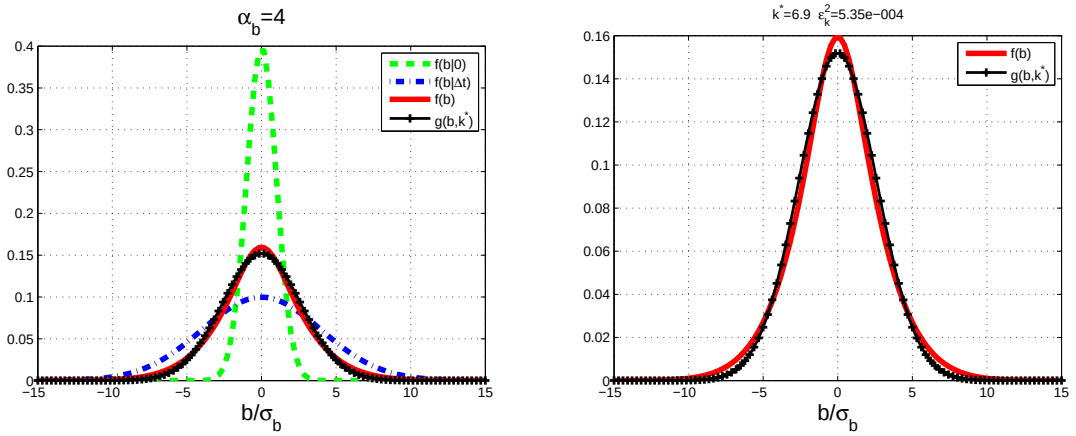

(a) Bias pdf dispersion

(b) Sampled bias pdf and matched Gaussian

Figure 4: Sampled clock bias model

Appendix 2- Static Multiple Model Estimator

The Static Multiple Model (SMM) [15] is an estimator of dynamic systems that can assume a finite number of modes. The actual system mode is unknown, however it is known that the mode is determined once with no following mode switching. Each system mode can be described by Eq.(113) and (114) with a set of known mode parameters at every time step $\mathcal{M}_k^i = \{F_k^i, G_k^i, \mathbf{u}_k^i, B_k^i, Q_k^i, R_k^i\}$:

$$\mathbf{x}_{k+1}^i = F_k^i \mathbf{x}_k + G_k^i \mathbf{u}_k^i + B_k^i \mathbf{w}_k^i \tag{113}$$

$$\mathbf{z}_k = H_k \mathbf{x}_k^i + \mathbf{v}_k^i \tag{114}$$

At every time step each mode is given an a priori probability μ_k^i of being the correct systems mode. A Kalman filter corresponding to the set of mode parameters is used to obtain the posterior estimate shown in Eq.(115) and (118) and to calculate the mode likelihood. In the case of a nonlinear model, an EKF is used for each mode.

$$\hat{\mathbf{x}}_{k+1}^i = \left(I - K_{k+1}^i H_{k+1}\right)\left(F_k^i \hat{\mathbf{x}}_k^i + G_k^i \mathbf{u}_k^i\right) + K_{k+1}^i \mathbf{z}_{k+1} \tag{115}$$

$$S_{k+1}^i = H_{k+1} P_{k+1|k}^i H_{k+1}^T + R_{k+1}^i \tag{116}$$

$$K_{k+1}^i = P_{k+1|k}^i H_{k+1}^T \left(S_{k+1}^i\right)^{-1} \tag{117}$$

$$P_{k+1}^i = \left(I - K_{k+1}^i H_{k+1}\right) P_{k+1|k}^i \left(I - K_{k+1}^i H_{k+1}\right)^T + \left(K_{k+1}^i\right) R_{k+1}^i \left(K_{k+1}^i\right)^T \tag{118}$$

The mode likelihood is defined as the value of the conditional probability density function (**pdf**) for a given measurement $\Lambda_{k+1}^i \equiv f\left(\mathbf{z}_{k+1} | Z_k, \mathcal{M}_{k+1}^i\right)$. If the KF assumptions hold for all the modes then the SMM is the optimal estimator in a MMSE sense. In this case the conditional measurement **pdf** is normal with a mean that is equal to the mode matched innovation $\nu_{k+1}^i = \mathbf{z}_{k+1} - \hat{\mathbf{z}}_{k+1}^i$ and covariance $S_{k+1}^i = \mathrm{COV}\left\{\nu_{k+1}^i\right\}$. The mode likelihood is then [15]:

$$\Lambda_{k+1}^i = \left(\left|2\pi \cdot S_{k+1}^i\right|\right)^{-\frac{1}{2}} \exp\left[-\frac{1}{2}\left(\nu_{k+1}^i\right)^T \left(S_{k+1}^i\right)^{-1} \left(\nu_{k+1}^i\right)\right] \tag{119}$$

The a priori mode probabilities and the likelihood of each mode are used to update the mode probabilities:

$$\mu_{k+1}^i = \frac{1}{c} \cdot \Lambda_{k+1}^i \cdot \mu_k^i \tag{120}$$

$$c = \sum_{j=1}^{m} \Lambda_{k+1}^j \cdot \mu_k^j \tag{121}$$

The updated state estimate (122) and covariance (123) are the mixture equations of the mode estimations [15]:

$$\hat{\mathbf{x}}_{k+1|k+1} = \sum_{j=1}^{m} \mu_{k+1}^j \cdot \hat{\mathbf{x}}_{k+1|k+1}^j \tag{122}$$

$$P_{k+1|k+1} = \sum_{j=1}^{m} \mu_{k+1}^j \cdot \left[P_{k+1|k+1}^j + \left(\hat{\mathbf{x}}_{k+1|k+1}^j - \hat{\mathbf{x}}_{k+1|k+1}\right)\left(\hat{\mathbf{x}}_{k+1|k+1}^j - \hat{\mathbf{x}}_{k+1|k+1}\right)^T\right] \tag{123}$$